



OPEN Identification and validation of hub genes associated with biotic and abiotic stresses by modular gene co-expression analysis in *Oryza sativa* L.

Izreen Izzati Razalli¹, Muhammad-Redha Abdullah-Zawawi²✉, Rabiatul Adawiah Zainal Abidin³, Sarahani Harun⁴, Muhamad Hafiz Che Othman¹, Ismanizan Ismail¹ & Zamri Zainal^{1,4}✉

Rice, a staple food consumed by half of the world's population, is severely affected by the combined impact of abiotic and biotic stresses, with the former causing increased susceptibility of the plant to pathogens. Four microarray datasets for drought, salinity, tungro virus, and blast pathogen were retrieved from the Gene Expression Omnibus database. A modular gene co-expression (mGCE) analysis was conducted, followed by gene set enrichment analysis to evaluate the upregulation of module activity across different stress conditions. Over-representation analysis was conducted to determine the functional association of each gene module with stress-related processes and pathways. The protein–protein interaction network of mGCE hub genes was constructed, and the Maximal Clique Centrality (MCC) algorithm was applied to enhance precision in identifying key genes. Finally, genes implicated in both abiotic and biotic stress responses were validated using RT-qPCR. A total of 11, 12, 46, and 14 modules containing 85, 106, 253, and 143 hub genes were detected in drought, salinity, tungro virus, and blast. Modular genes in drought were primarily enriched in response to heat stimulus and water deprivation, while salinity-related genes were enriched in response to external stimuli. For the tungro virus and blast pathogen, enrichment was mainly observed in the defence and stress responses. Interestingly, *RPS5*, *PKG*, *HSP90*, *HSP70*, and *MCM* were consistently present in abiotic and biotic stresses. The DEG analysis revealed the upregulation of *MCM* under the tungro virus and downregulation under blast and drought in resistant rice, indicating its role in viral resistance. *HSP70* showed no changes, while *HSP90* was upregulated in susceptible rice during blast and drought. *PKG* increased during drought but decreased in japonica rice under salinity. *RPS5* was highly upregulated during blast in both resistant and susceptible rice. The RT-qPCR analysis showed that all five hub genes were upregulated in all treatments, indicating their role in stress responses and potential for crop improvement.

Keywords Modular gene co-expression, Hub genes, Drought, Salinity, Tungro virus, Blast pathogen

Abbreviations

ROS	Reactive oxygen species
RTD	Rice tungro disease
RTBV	Rice tungro bacilliform virus
RTSV	Rice tungro spherical virus
mGCE	Modular gene co-expression

¹Faculty of Science and Technology, Universiti Kebangsaan Malaysia (UKM), 43600 Bangi, Selangor, Malaysia.

²UKM Medical Molecular Biology Institute (UMBI), Universiti Kebangsaan Malaysia, Jalan Ya'acob Latiff, Bandar Tun Razak, 56000 Cheras, Kuala Lumpur, Malaysia. ³Biotechnology & Nanotechnology Research Centre, Malaysian Agricultural Research and Development Institute (MARDI), 43400 Serdang, Selangor, Malaysia.

⁴Institute of Systems Biology, Universiti Kebangsaan Malaysia (UKM), 43600 Bangi, Selangor, Malaysia. ✉email: mrz@ukm.edu.my; zz@ukm.edu.my

GSEA	Gene set enrichment analysis
ORA	Over-representation analysis
PPI	Protein–protein interaction
GO	Gene ontology
RT-qPCR	Quantitative reverse transcription polymerase chain reaction
GEO	Gene Expression Omnibus
FTSW	Fraction of transpirable soil water
PCC	Pearson correlation coefficient
FGSEA	Fast gene set enrichment analysis
NES	Normalised enrichment score
BP	Biological process
MF	Molecular function
CC	Cellular component
FDR	False-discovery rate
KEGG	Kyoto Encyclopedia of Genes and Genomes
MCC	Maximal clique centrality
DEG	Differentially expressed gene
ABA	Absciscic acid
cGMP	Cyclic guanosine 3',5'-monophosphate
TCA	Tricarboxylic acid

Rice accounts for nearly 90% of worldwide production and is a staple food for most people globally¹. However, it is estimated that approximately 95% of crop losses can be attributed to the effects of climate change, emphasising the significant challenges faced by this agricultural commodity². Fluctuating temperatures can lead to an imbalanced impact on agricultural productivity, causing the convergence of numerous abiotic and biotic stressors, which can alarmingly impact rice growth and yield³. Continuous exposure to environmental stressors, such as drought and salinity, can lead to significant cellular damage and trigger various stress-induced phytotoxic effects in crops⁴. These conditions consequently weaken plant resilience, accelerate the life cycles of pests and pathogens, and disrupt their physiological and metabolic processes⁵.

In Malaysia, salinity poses a significant challenge for farmers, leading to notable incidents, such as the 2016 seawater inundation of 36 hectares of rice fields⁶. Salinity can induce oxidative stress by promoting the excessive generation of reactive oxygen species (ROS), disrupting plant metabolism, and significantly decreasing yield⁷. The aftermath of severe flooding during the early 2000s further exacerbated the situation, resulting in a substantial decline in rice production, estimated at around 75%, due to saline water intrusion in Kuala Kedah⁸.

Pathogen attacks resulting from post-abiotic stressors, including viral diseases such as rice tungro disease (RTD), have emerged as a significant burden, causing a 70% fall in yield⁹. RTD, initially identified as *penyakit merah* based on its signs and symptoms, had its first reported case in Sarawak in 1965¹⁰. Both rice tungro bacilliform virus (RTBV) and rice tungro spherical virus (RTSV) are challenging to detect in the field because their symptoms, such as stunted growth, orange discolouration of infected leaves, and irregularly shaped dark brown specks on the leaves resemble those caused by abiotic and biotic factors, rendering diagnosis a challenge⁹. Apart from RTD, rice blast, caused by the fungus *Magnaporthe oryzae*, is also considered the most devastating disease affecting rice crops in Malaysia, with two prevalent types of blast diseases commonly observed: foliar blast, which affects seedlings during their early growth stage, and panicle blast, which infects the panicles as they reach the reproductive stage¹¹.

Plants survive harsh conditions through effective defence mechanisms and signalling pathways that enhance their tolerance to abiotic and biotic stresses¹². Hence, it is essential to understand the adaptation strategies of agricultural plants to both biotic and abiotic stress to identify genes that play crucial roles in regulating the defence function under combined stress conditions¹³. Thus, deciphering shared pathways using omics data from various stress-related studies would benefit understanding universally regulated genes under combined and individual stress.

Transcriptome analysis has become a valuable approach in the post-genomic era to gain insights into the consequences of abiotic and biotic factors on regulating gene expression during transcription in cells. A deeper understanding of functional alterations at the transcript level is essential to characterise stress-related cellular and molecular changes comprehensively. Gene co-expression network analysis (GCNA) identifies functional key genes from high-throughput data generated through RNA-sequencing and microarray technology¹⁴. However, GCNA alone is challenging to interpret and prioritise the critical genes with known or unknown functions or a low number of hits. Therefore, combinatorial approaches, such as module and hub gene detection, are required to infer gene function. Co-expression modules encompass clusters of genes and are essential to identify the pivotal gene within each module responsible for the primary function. This is achieved by pinpointing highly interconnected genes, commonly called hub genes, which often play a more significant role in regulating the functionality of the network¹⁵. Modules assist in identifying hub genes that may act as regulators, controlling other essential genes under specific phenotypes, and provide valuable insights into understanding the underlying mechanisms¹⁶. Gene sets within the same co-expression modules are often associated with the same category, participate in similar biological processes, or are components of the same pathway^{17,18}.

To date, several studies have reported the application of modular gene co-expression (mGCE) in rice. For instance, Ramkumar et al.¹⁹ performed a meta-analysis of microarray data against multiple abiotic stress tolerance (drought, heat, and salinity stresses) in rice at the seedling stage. They identified 10 modules and revealed 10 genes (e.g., LOC_Os05g47890, LOC_Os02g32590, and LOC_Os01g04330) common to the three abiotic stresses studied. Another mGCE analysis reported by Zhang et al.²⁰ investigated agronomic trait-related

genes (i.e., grain size, grain number, stem strength, anthocyanin content) in rice. They showed that rice trait genes typically form modules within GCE analysis, indicating that the trait-associated modules may help the identification of additional trait genes²⁰. Some genes associated with plant hormone biosynthesis and signal transduction were pinpointed by modules of rice against cold stress in the 9311 and DC907 rice cultivars²¹. Additionally, Sharma et al.²² identified 15 co-expression modules comprising nitrogen-responsive genes in rice, prioritising 7 genes related to nitrogen response and nitrogen use efficiency (NUE) for RT-qPCR analysis. Recently, Azad et al. (2024) investigated several abiotic stresses (i.e., salinity, drought, heat and cold stress, and nitrogen starvation) in rice²³. They found six modules associated with multiple abiotic stresses via weighted gene co-expression network analysis (WGCNA) and validated five genes (*TIFY9*, *RAB16B*, *ADF3*, *Os01g0124650*, and *Os05g0142900*) using qRT-PCR. Most studies have employed WGCNA, which offers limited options for functional analysis²⁴. However, a previous study demonstrated that mGCE analysis using CEMiTool outperforms other tools like WGCNA and Coseq²⁵. CEMiTool is more reproducible and user-friendly compared to WGCNA, which has a more complex pipeline, and Coseq, which lacks the ability to identify gene targets²⁵.

The present study utilised four microarray datasets of abiotic stress (drought and salinity) and biotic stress (RTD and blast pathogen) retrieved from the database of Gene Expression Omnibus (GEO). The mGCE analysis was executed on samples obtained from various conditions to identify key genes responsible for combined stresses. Subsequently, Gene Set Enrichment Analysis (GSEA) was employed to ascertain the module activity for each group of samples. This was followed by constructing a gene network, over-representation analysis (ORA) of pathways and gene ontology (GO) and identifying the top ten highly connected genes. The selected hub genes were subsequently validated on samples subjected to drought, salinity, blast pathogen, and tungro virus treatments. This validation was carried out using RT-qPCR to assess their potential roles in responding to the respective abiotic and biotic stresses. The uniqueness of this study lies in its integration of abiotic and biotic stresses, i.e., common genes and pathways that are activated and expressed under all four stress conditions (drought, salinity, RTD, and blast).

Materials and methods

Data collection and pre-processing

A simplified overview of this study is demonstrated in Fig. 1. The gene expression microarray datasets of drought, salinity, tungro virus, and blast pathogen were retrieved from the GEO database (<https://www.ncbi.nlm.nih.gov/geo/>)²⁶. For drought stress, 30 samples were downloaded from GSE30449, comprising two drought-resistant and three drought-susceptible genotypes, with 15 samples for each treatment of 0.2 and 0.5 FTSW (Fraction of Transpirable Soil Water)²⁷. Meanwhile, salinity (GSE79043) included 46 samples from 8 different rice genotypes under the treatments of 0 mM ($n=23$) and 120 mM ($n=23$) NaCl concentrations²⁸. The GSE16142 dataset for the tungro virus was obtained from a study by Lee et al., where 12 susceptible (TN1) and 9 resistant (TW16) rice samples were infected by RTSV at different growth lengths²⁹. Subsequently, the blast pathogen dataset, GSE62422, was downloaded from the study by Tanabe et al. (2014)³⁰. It comprised 12 resistant and 12 susceptible rice samples, which were treated with rice blast fungus every 12 h for 2 days. The mRNA expression data of GSE30449 and GSE16142 were obtained by the Custom GER rice oligoarray platform, while GSE79043 and GSE62422 were obtained from the Agilent-015241 Rice Gene Expression 4 × 44 K platform. Due to the duplication of gene symbols identified among the unique probe identifiers, their mean values were calculated and regarded as the ultimate gene expression values. Probes that did not match the corresponding gene identity were discarded to ensure that the probes used to construct the mGCE were fully annotated with known functions.

Modular gene co-expression analysis

The pre-processed gene expression dataset was merged into a single matrix based on stress type for input and then transformed into a gene expression matrix of dimensions ($m \times n$), where 'm' represents genes and 'n' represents samples. The Pearson Correlation Coefficient (PCC) was employed to calculate the correlation between the genes using CEMiTool²⁴. The modules were constructed using the following parameters: (i) a coefficient of determination for linear regression fit ($R^2 \geq 0.8$), (ii) a minimum number of genes in a module ($\text{min_ngen} \geq 20$), (iii) a threshold similarity of eigengene ($\text{diss_thresh} \geq 0.8$), (iv) correlation method = PCC, and (v) the identification of a set number of highly connected genes in each module, referred to as hub genes ($n = 10$). Modules with an adjusted p -value ≤ 0.05 were considered significant.

Gene set enrichment analysis (GSEA) of mGCE activity

The mGCE activity was evaluated using the efficient Fast Gene Set Enrichment Analysis (FGSEA) R function integrated within CEMiTool, where the up and downregulated modules between classes were determined³¹. The genes derived from mGCE were employed as discovery sets for this analysis. The mGCE activity was generated based on the Normalised Enrichment Score (NES), representing a module's enrichment score for each class and normalised by the module's number of genes. The gene set size, representing the genes within each module, was generated within a default range of 15 to 1000.

Over representation analysis (ORA)

The ORA analysis of mGCE was conducted using the ClusterProfiler R package³². The GO information for biological processes (BP), molecular functions (MF), and cellular components (CC) of the significantly upregulated modules was obtained from Phytozome (<https://phytozome-next.jgi.doe.gov/>)³³ and Oryzabase (<https://shigen.nig.ac.jp/rice/oryzabase/>)³⁴ prior to conducting the enrichment analysis. The parameters used for ORA included an adjusted p -value threshold of < 0.05 , a minimum gene set size (minGSSize) of 3, a maximum gene set size (maxGSSize) of 800, and the false-discovery rate (FDR) as the statistical correction method³⁵.

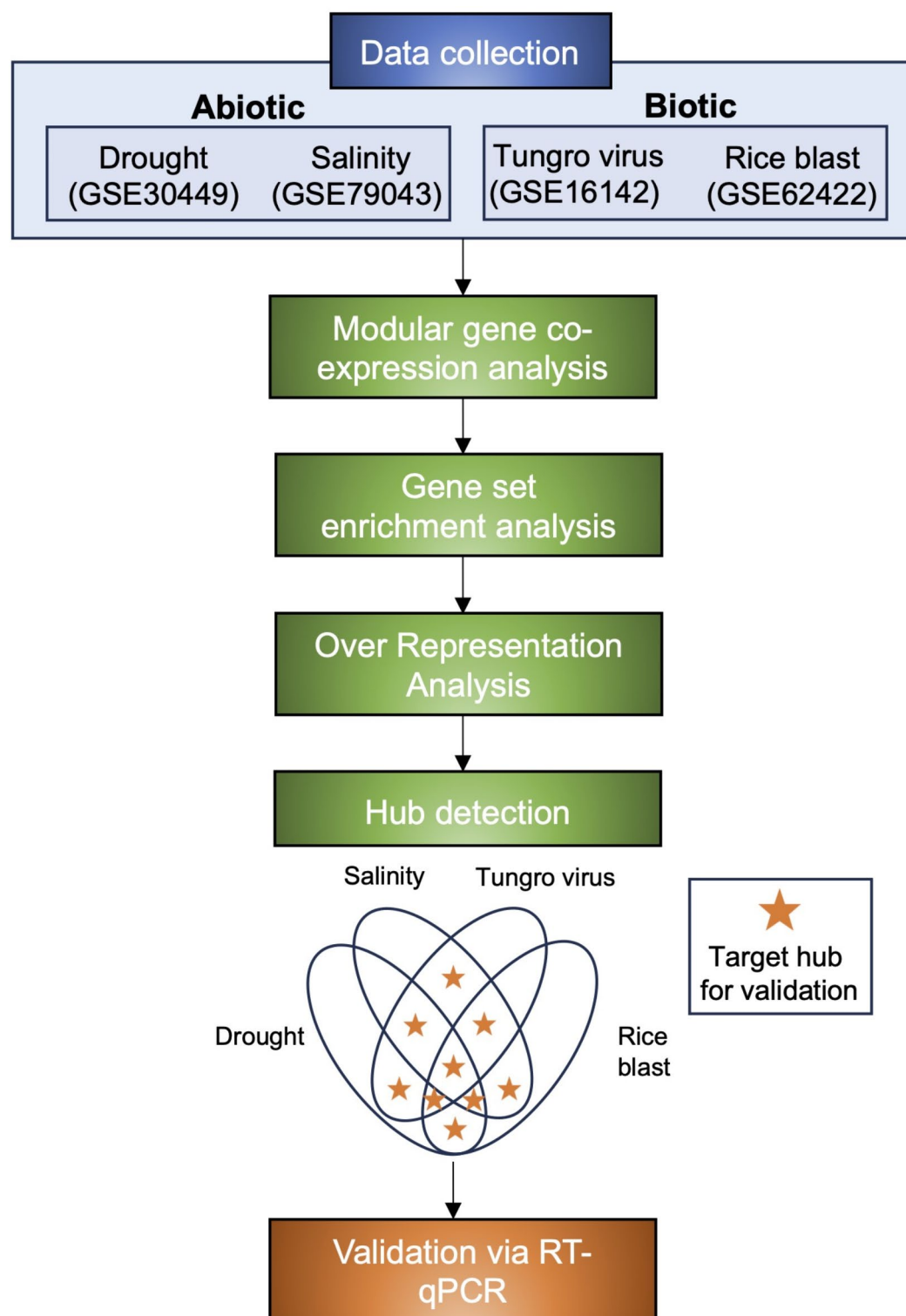


Fig. 1. A simplified overview of the study. This study involved the collection of expression data from the Gene Expression Omnibus, followed by computational analyses, including mGCE, gene set enrichment analysis, over-representation analysis, and hub gene detection. The target hub genes present in both abiotic and biotic conditions were considered for validation via RT-qPCR.

KEGG pathway mapping

For pathway mapping analysis of each mGCE, the study utilised the KEGG Mapper tool version 4.3 (<https://www.genome.jp/kegg/mapper.html>)³⁶. The genes within each mGCE were then classified into several KEGG pathway categories, including (i) metabolism, (ii) genetic processes, (iii) environmental information processing, (iv) cellular processes, and (v) organismal systems.

Construction of mGCE-based protein–protein interaction and hub gene detection

The network was constructed using the mGCE in conjunction with a priori PPI information retrieved from the STRING database to understand the interaction involving the mGCE³⁷. The PPI dataset for each module was retrieved using the Cytoscape plug-in StringApp³⁸. The protein identity of mGCE was queried against the STRING human interaction database with a confidence score cutoff of 0.4 and a maximum of 0 additional interactors. During the pre-processing, a single protein without interactions was excluded, and only known interactions from curated databases and experimentally derived interactions were considered for the subsequent analyses. The network was then visualised using Cytoscape software. The cytoHubba plug-in was used to determine the highly interacted genes, best known as hub genes³⁹. The Maximal Clique Centrality (MCC) algorithm was applied due to its improved precision in predicting important genes from the network³⁹. Meanwhile, GEO2R (<https://www.ncbi.nlm.nih.gov/geo/geo2r/>) was utilised to identify the differentially expressed genes (DEGs) to determine the roles of hub genes in resistance and susceptibility under stress conditions⁴⁰. The parameters employed were as follows: $|\text{Log}_2\text{FC}| > 1$, p -adjust value < 0.05 , and the Benjamini and Hochberg method was applied to correct false positive results. The Euclidean clustering heatmap of expression profiles was then generated using the Ward clustering method in ClustVis (https://biit.cs.ut.ee/clustvis_large/)⁴¹. The genes detected as the hubs in both abiotic and biotic stresses were selected for further validation in response to drought, salinity, blast pathogen, and tungro virus treatments via RT-qPCR.

Plant materials and stress treatments

All experiments were conducted in a glasshouse facility at Universiti Kebangsaan Malaysia (UKM) under ambient conditions. Glasshouse temperatures ranged from 28 to 38 °C during the day and 22–26 °C at night, with relative humidity fluctuating between 50 and 85%. Natural light was utilised, with a photoperiod approximating 12 h of daylight and 12 h of darkness. These environmental conditions were applied uniformly to both the control and treated groups to ensure consistency.

Drought treatment

For drought treatments, pots were filled with a predetermined weight of potting mixture, thoroughly watered to saturation, and left to drain overnight to simulate field capacity. Fourteen-day-old rice seedlings (MR219) were subjected to drought stress (without watering) at 0, 12, 24, 48, and 96 h. Three biological replicates were collected for every time point to ensure reproducibility. Leaves were promptly immersed in liquid nitrogen and stored at -80 °C for RNA extraction.

Salinity treatment

Fourteen-day-old rice seedlings (MR219) were subjected to salinity stress by exposing the root to varying concentrations of NaCl (0 and 120 mM) at two specific time points: 24 h and 120 h, following the method described by Hossain et al.²⁸. At every time point, three biological replicates were collected to ensure reproducibility. For RNA extraction, leaves were directly immersed in liquid nitrogen and stored at -80 °C.

Blast infection

The *M. oryzae* isolate was obtained from blast pathogen infections at the Faculty of Science and Technology, UKM. The treatment for rice blast followed the procedure outlined by Hayashi and colleagues⁴². Oatmeal agar plates were used to cultivate *M. oryzae*, grown at 30 °C. A conidia suspension (fungal spores) was prepared at 1×10^6 spores/mL. Subsequently, the conidia suspension was sprayed onto the fourth leaf of rice plants, which were kept in darkness at 25 °C for 24 h. Afterwards, the plants were transferred to a growth chamber with a 14-h light cycle at 28 °C and a 10-h dark cycle at 24 °C for a maximum of 5 days. In the control group, water was sprayed on the rice leaves, and these control plants underwent the same procedures as described above. Three biological replicates were gathered from control and treated plants. Leaves were promptly immersed in liquid nitrogen and stored at -80 °C for RNA extraction.

Tungro virus infection

Fourteen-day-old rice plants were cultivated in pots and placed close to a plot that was already affected by tungro disease-associated viruses, including RTBV and RTSV. These viruses are primarily transmitted from plant to plant by leafhoppers. Pathogens can invade the plant through natural openings or wounds by contacting its surface. Hence, to achieve comprehensive infection, infected leaves that consistently displayed signs of the disease were gently used to rub the untreated plants in the pots. The infection exposure was conducted at two distinct time points: ten days and one month after planting. Three biological replicates were collected from control and infected plants. Leaves were right away immersed in liquid nitrogen and stored at -80 °C to extract the RNA.

Total RNA isolation and validation through RT-qPCR

RNA was extracted from leaf tissues for drought, salinity, tungro virus, and blast pathogen treatments. TRIzol® reagent was used, followed by DNase treatment (Ambion® TURBOTMTM). Total RNA was reverse transcribed into cDNA using the Maxima kit from Thermo Fisher. Equal amounts of cDNA were used for PCR with SYBR

Green Master Mix from Thermo Fisher. Gene-specific primers, actin and U6, were used as controls. PCR reactions were performed in 20 μ L volumes with a specific cycling protocol. Melting curves were used to assess specificity. Real-time PCR was performed on the three biological replicates and analysed using the $2^{-\Delta\Delta C_t}$ method. Efficiency and Ct values were analysed using LinRegPCR. The Livak method was employed for relative expression analysis⁴³.

Results

Modular analysis of drought, salinity, tungro virus, and blast pathogen

In this study, mGCE analysis was conducted to explore the genes that play a significant role in rice defence responses against abiotic and biotic stresses. For drought, 11 modules were identified using CEMiTool, containing 3962 genes in rice drought-resistant (IR77298A and IR77298C) and drought-susceptible (IR77298B and IR77298D). Six modules were discovered to be associated with drought response, such as M3, M4, M6, M7, M9, and M11. The activities of modules M4 (NES = 2.96) and M11 (NES = 3.15) were found to be strongly upregulated in drought-resistant rice, while M7 (NES = 3.44) and M9 (NES = 3.05) were strongly upregulated in drought-susceptible rice. Modules M3 and M6 were upregulated in both resistant (NES = 3.4) and susceptible (NES = 2.66) (Fig. 2; Supplementary Table 1a). For salinity, 3238 genes from 12 modules were discovered. Under the 0 and 120 mM NaCl treatments, modular genes from the japonica genotype were noted to respond the most to salt stress, in concordance with the upregulation activities of M2, M3, M6, M8, and M12, compared to the wild-type (M3) and indica (M7) genotypes. Among these modules, M2 exhibited the highest number of genes ($n = 479$) and strongly upregulated with NES = 5.72 in japonica, followed by M3 ($n = 221$; NES = 3.88) and M12 ($n = 24$; NES = 3.35). In the wild-type group, eight out of nine mGCE activities were found to be downregulated, except for M3, while in the indica group, only M7 was observed to be upregulated (Fig. 3; Supplementary Table 1b). It is suggested that japonica is more susceptible to salinity than wild-type and indica.

For biotic stress, 46 modules were identified from datasets subjected to tungro virus treatment, involving 4259 genes. However, only 15 were known to be significant, as the p-adjusted value was < 0.05 (Fig. 4; Supplementary Table 1c). Overall, the susceptible group (TN1) showed a general downregulation across the modules, except for M4 and M15, with an NES of 2.6. In contrast, the resistant group (TW16) displayed upregulation trends in most modules, except in M4 (NES = -2.62), M8 (NES = -1.8), and M14 (NES = -2.6). In the TW16 group, M15 was highly upregulated (NES = 3), followed by M21 (NES = 71) and M6 (NES = 2). Based on these results, it is postulated that genes in the upregulated modules of TW16 could play important roles in rice protection against the tungro virus. However, further validation is needed to infer their function. Five significant modules for blast pathogen, specifically M2, M3, M6, M11, and M14, have been identified from 14 modules (Fig. 5 and Supplementary Table 1d). Notably, M2 and M3 each harboured the highest gene counts, boasted 732 and 519, respectively, and M2 (NES = 1.7) and M11 (NES = 1.85) exhibited upregulation in the resistant group, while M6 (NES = 2.82) and M14 (NES = 1.69) showed an upregulation in the susceptible group. Considering the upregulated module information, it is hypothesised that these genes might be important in activating responses to various stresses, ultimately leading to accurately identifying target genes under combined stress conditions.

Over representation analysis

An ORA was performed to identify potential biological functions associated with each module. Among these, drought:M2 has shown significant associations with responses to water deprivation, salt stress, abscisic acid (ABA) stimulus, and ABA signalling. M2 was significantly enriched in susceptible rice varieties (IR64 and IR77298D), and the upregulation of M2 in IR64 suggests that this variety is more sensitive to drought response than IR77298D (Fig. 2c,d). For the tungro assessment, M1 refers to RNA binding, protein folding, nucleolus, and mitochondrion, while another significantly enriched module is M6, which is associated with the response to ABA stimulus, water, salt stress, water deprivation, and hydrogen peroxide, and M7 is linked the lipid metabolic process. The involvement of tungro:M6 in response to water and salinity-related stress suggests that M6 could be a potential mGCE that participates in combined stresses (Fig. 4c,e). Additional enrichment analyses were performed on mGCE data from the blast pathogen and salinity datasets using the STRING database due to the lack of significant hits in the clusterProfiler output. Interestingly, stress-related reactions, such as response to stimuli, stress response, defence mechanisms, phenylpropanoid metabolic processes, and biogenesis, were also enriched among the blast:M2 and blast:M3 genes. For salinity, the mGCE refers to responses to biotic stimuli, other organisms, external stimuli, fungi, and terpenoid metabolic processes. The presence of biotic processes in the salinity dataset suggests the potential involvement of these genes in responding to attacks from microorganisms.

Hub genes in mGCE

The top 10 hub genes were detected from each module using the MCC algorithms of cytoHubba across salinity, drought, tungro, and blast (Table 1). Within the 11 drought stress modules (M1 to M11), 86 genes were discovered, with resistance to *Pseudomonas syringae* 5 (RPS5), homeodomain-leucine zipper class 2 transcription factor F (*OsHAP2F*), eukaryotic translation initiation factor 4E isoform (*EIFISO4*), Daikoku dwarf (*D1*), polypentenyltransferase 1 (*PPT1*), heat-shock protein 90 (*HSP90*), G-box factor 14-3-3b protein (*GF14B*), ARF-like protein 1a (*ARL1A*), gibberellin-insensitive dwarf protein 2 (*GF14E*), and electron transfer flavoprotein subunit alpha (*ETFA*) detected as the top 10 hubs. In salinity, 106 genes were found across 12 modules, revealing the top 10 hub genes: late embryogenesis abundant protein 16 (*LEA16*), late embryogenesis abundant protein 17 (*LEA17*), mini-chromosome maintenance protein 2 (*MCM2*), cell division control 45-1 (*CDC45-1*), Aurora-B, Os10g0505900, cytochrome c, Zinc finger CCCH domain-containing protein 43 (*C3H43*), heat shock protein 70 (*HSP70*), and protein phosphatase 23 (*PKG*). For the tungro virus, the top 10 hub genes, including retinoblastoma-related protein-2 (*RBR2*), cyclin-dependent kinase A1 (*CDKA-1*), 71.1

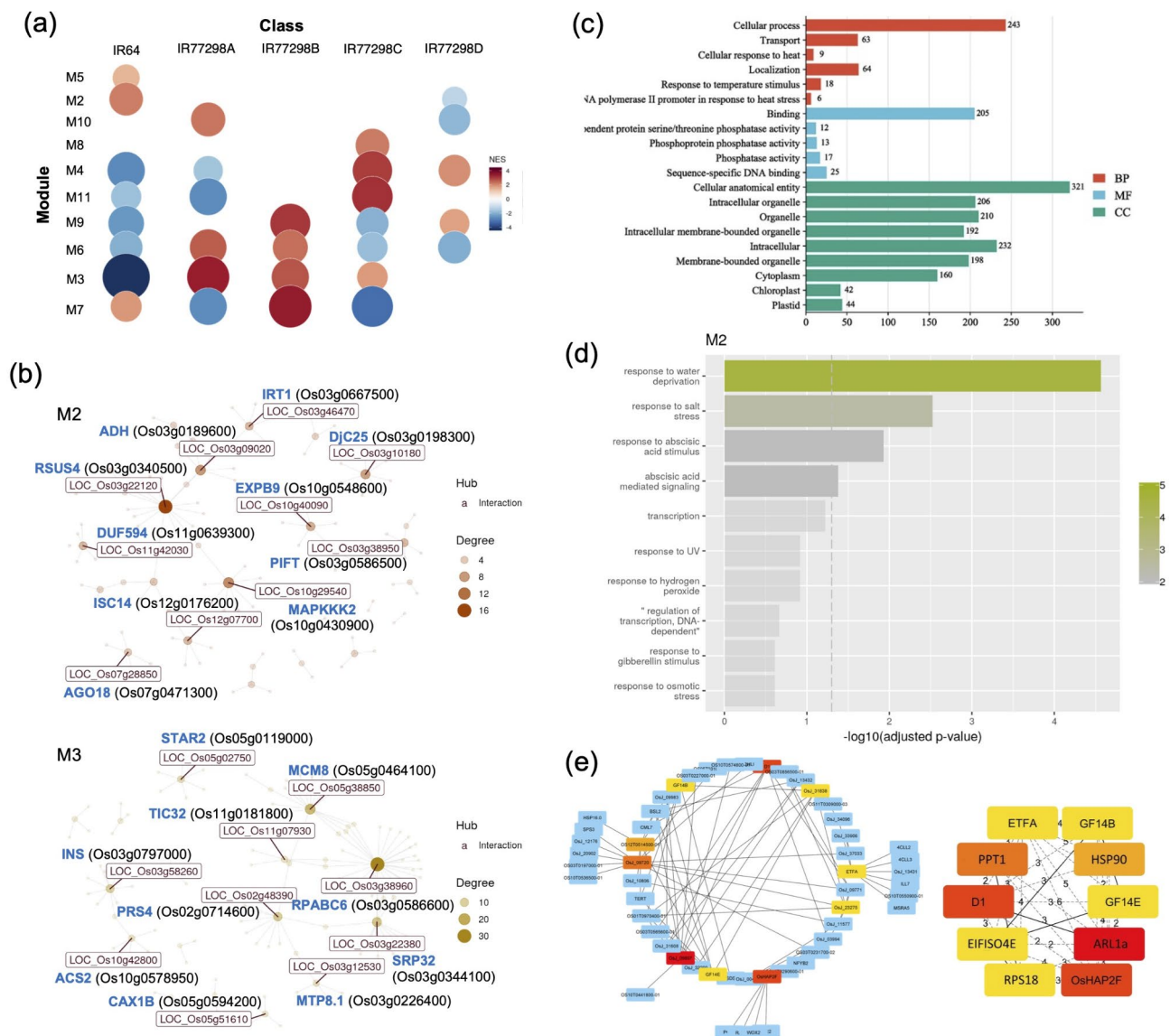


Fig. 2. Identification of important gene modules under drought condition via mGCE analysis: **(a)** GSEA depicts module activity across different genotypes: “IR77298A and IR77298C” (drought-resistant) and “IR77298B, IR77298D, and IR64” (drought-susceptible), generated using CEMiTool v1.30.0. The blue circle represents the downregulated gene module, and the red circle denotes the upregulated gene module; **(b)** mGCE-based PPI networks for modules M2 and M3. The top 10 genes are labelled and color-coded based on their origin: blue for genes from the CEMiTool module and red for those from the STRING interactions file. Node size corresponds to the degree of interactions; **(c)** GO enrichment analysis for hub genes across all modules (M1–M11); **(d)** ORA demonstrates the overrepresented processes among gene module M2; and **(e)** PPI network showing 85 hub genes collected from all modules, with the top 10 subsequently determined using the MCC algorithm.

kda class I heat shock protein (*HSP71.1*), heat-shock protein 90 (*HSP90*), Botrytis susceptibility 2 (*BSL2*), heat shock protein 70kd (*HSP70*), SPL11 cell-death suppressor (*SDS*), cyclin-B2-2 G2/mitotic-specific cyclin-B2-2 (*CYCB2-2*), mini-chromosome maintenance protein 4 (*MCM4*), and eukaryotic initiation factor 4E (*eIF4E*), were identified among 252 hub genes from 46 modules. Several essential hub genes in the blast pathogen also played crucial roles in plant defence response. For example, of 143 hub genes, ribosomal protein S8 (*RPS8*), ribosomal protein L4 (*RPL4*), metalloendopeptidase M24, ribosomal protein S5 (*RPS5*), PKG, nuclear protein H2 (*NHP2*), ribosomal protein L7 (*RPL7*), ribosomal protein S7 (*RPS7*), ribosomal protein L12 (*RPL12*) were discovered to be the top 10 hubs that respond to the blast pathogen.

All top hub genes were integrated from four different stressors—drought, salinity, tungro virus, and blast pathogen—to identify the key genes that play a crucial role in response to combined stresses, according to their highest connectivity scores (Table 2). It was shown that five hubs were identified as the central regulators in at least two different stress conditions (Supplementary Table 2, Fig. 6a). For instance, the involvement of *RPS5*

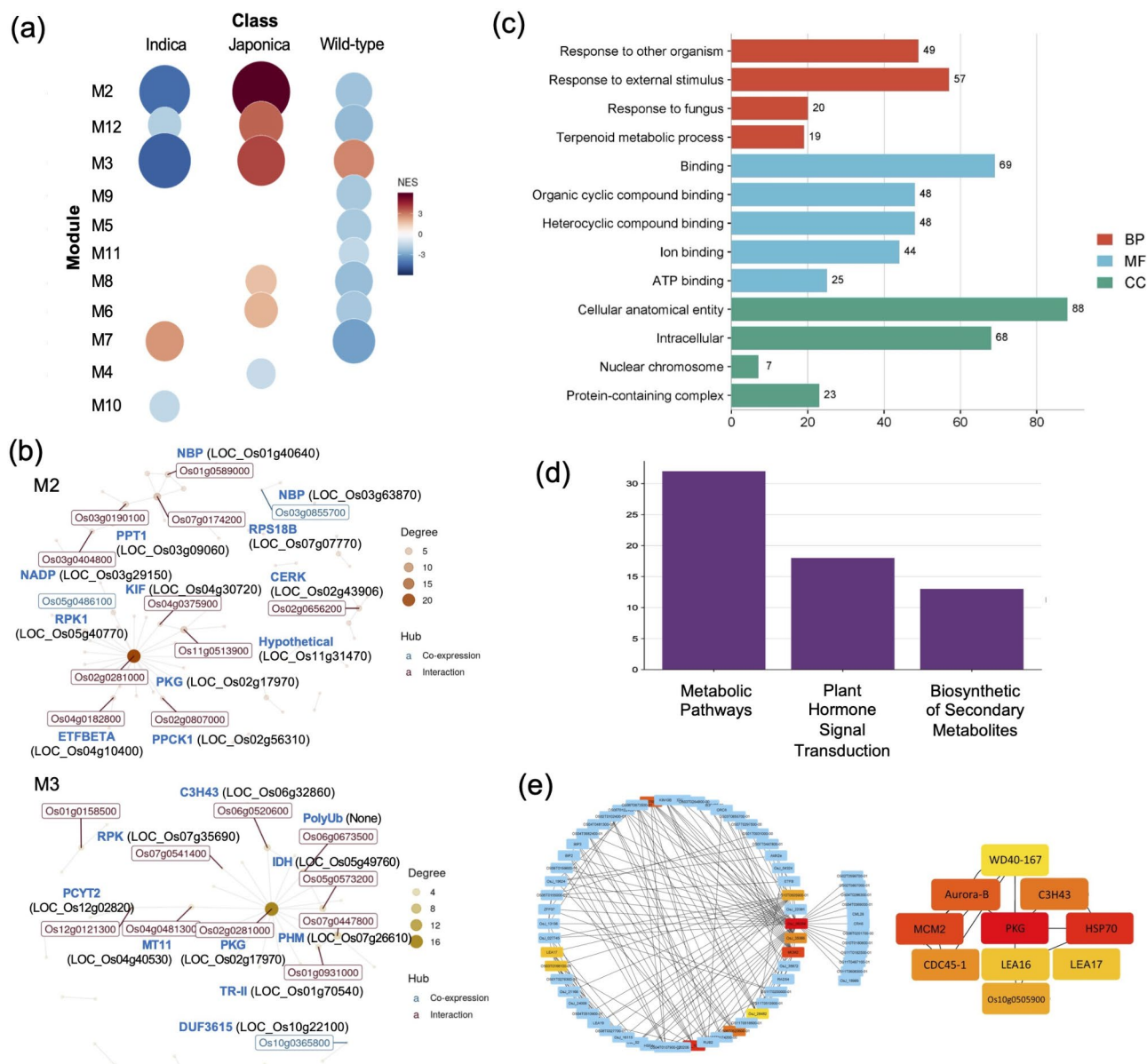


Fig. 3. Identification of important gene modules under salinity condition via mGCE analysis: (a) GSEA depicts module activity across Indica, Japonica, and Wild-type group, generated using CEMiTool v1.30.0. The blue circle represents the downregulated gene module, and the red circle denotes the upregulated gene module; (b) mGCE-based PPI networks for modules M2 and M3. The top 10 genes are labelled and color-coded based on their origin: blue for genes from the CEMiTool module and red for those from the STRING interactions file. Node size corresponds to the degree of interactions; (c) GO enrichment analysis for hub genes across all modules (M1–M12); (d) Bar graph demonstrates enriched KEGG pathways involving hub genes; and (e) PPI network demonstrates 106 hub genes identified from all modules, with the top 10 subsequently determined using the MCC algorithm.

in drought and blast pathogen, *HSP90* in drought and tungro virus, *MCM* in salinity and tungro, *HSP70* in salinity and tungro, and *PKG* in salinity and blast. All five genes were identified as differentially expressed across various stress scenarios to better understand the role of hub genes in resistance and susceptibility under stress conditions. Notably, *HSP90* exhibited high expression levels in the blast-resistant rice at 24, 36, and 48 h, while in the blast-susceptible rice, it was expressed only at 48 h, suggesting that rice becomes more susceptible to blast following prolonged exposure.

Additionally, during the tungro virus infection, *HSP90* was expressed early in both tungro-resistant and tungro-susceptible rice. It was also observed in drought-susceptible rice under drought stress (Supplementary Fig. 1). Similarly, *RPS5*, *HSP70*, *PKG*, and *MCM* exhibited high expression levels during blast and tungro virus infections, as well as under drought stress, in both resistant and susceptible rice varieties. Meanwhile, under salinity, *MCM*, *HSP70*, and *HSP90* were highly expressed in the wild-type group compared to *PKG* and *RPS5* in

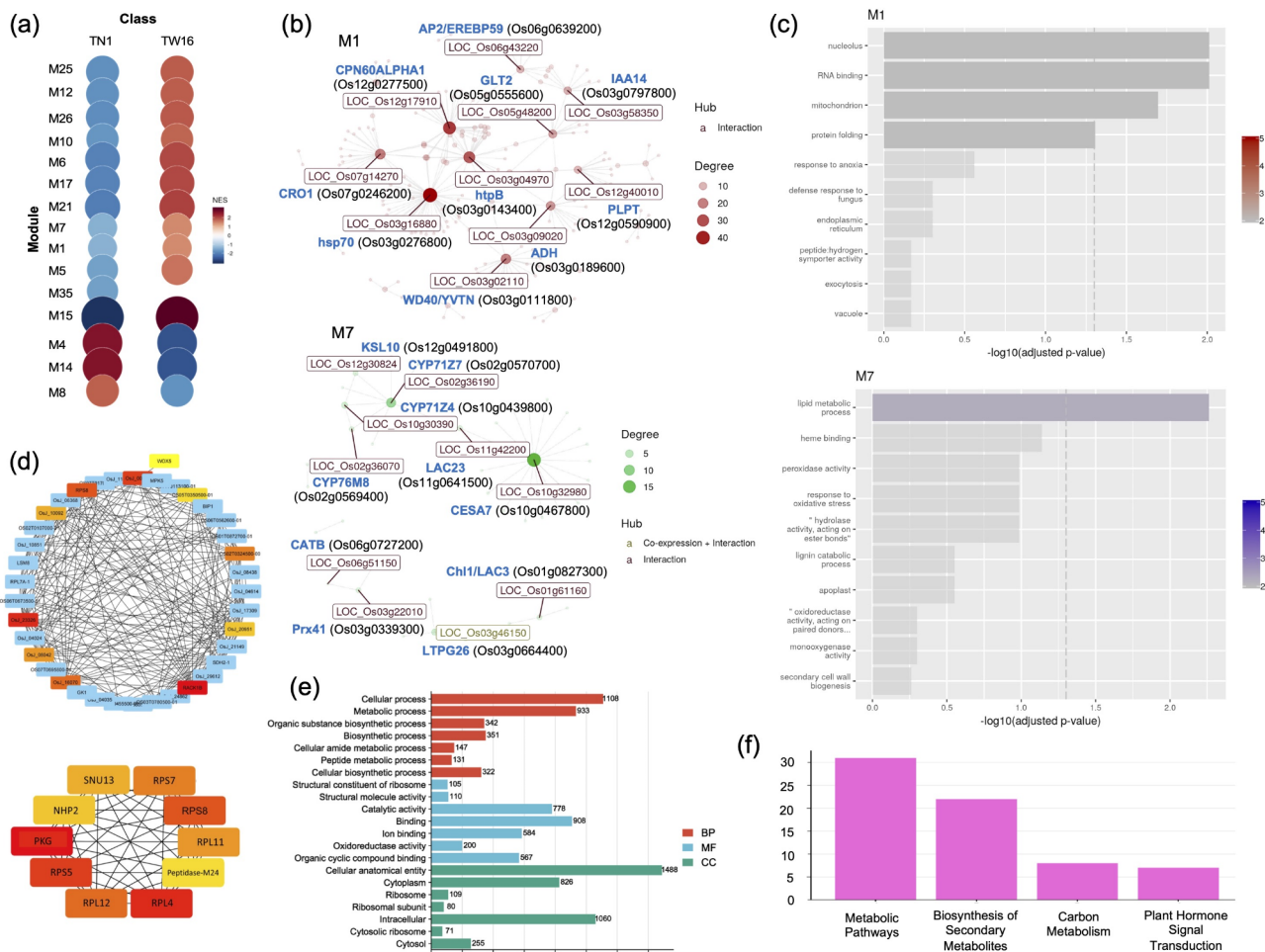


Fig. 4. Discovery of important gene modules under tungro virus infection via mGCE analysis: **(a)** GSEA depicts module activity of each class. “TN1”=susceptible and “TW16”=resistant, generated using CEMiTool v1.30.0. The blue circle represents the downregulated gene module, and the red circle denotes the upregulated gene module; **(b)** mGCE-based PPI networks for modules M1 and M7. The top 10 genes are labelled and color-coded based on their origin: blue for genes from the CEMiTool module and red for those from the STRING interactions file; **(c)** ORA of gene modules M1 and M7; **(d)** PPI network demonstrates 253 hub genes identified from all modules, with the top 10 subsequently determined using the MCC algorithm. **(e)** GO enrichment analysis for hub genes across all modules (M1–M46); and **(f)** Bar graph demonstrates enriched KEGG pathways involving hub genes.

indica and japonica rice. Differential expression analysis revealed that *MCM* was significantly upregulated under tungro virus conditions and downregulated under blast and drought conditions in resistant rice, highlighting its crucial role as a resistance gene against the virus. In contrast, *HSP70* showed no significant expression changes across treatments, while *HSP90* was upregulated in susceptible rice during blast infection and drought. Notably, *MCM* was downregulated in resistant rice under blast conditions and in both susceptible and resistant rice under drought conditions. Additionally, *PKG* expression was upregulated in susceptible and resistant rice during drought but downregulated in japonica rice under salinity stress. Finally, *RPS5* was highly upregulated in response to blast infection in both resistant and susceptible rice. RT-qPCR analysis was performed on *HSP90*, *HSP70*, *PKG*, *RPS5*, and *MCM* to validate these findings and assess their potential roles in abiotic and biotic stress.

Pathway analysis of mGCE hub genes

The hub genes for each module under different stress types were mapped onto KEGG pathways to determine their association with stress-related pathways. The pathway maps were grouped into five groups: genetic information processing, metabolism, cellular processes, environmental information processing, and organismal systems (Fig. 6b). Three pathways were associated with hub genes of the drought mGCE, including terpenoid biosynthesis, biosynthesis of secondary metabolites, and metabolic pathways. The salinity dataset demonstrated a strong association with environmental information processing, particularly in plant-pathogen interaction involving three hub genes. Additionally, the hub modules in the tungro virus displayed strong connections with

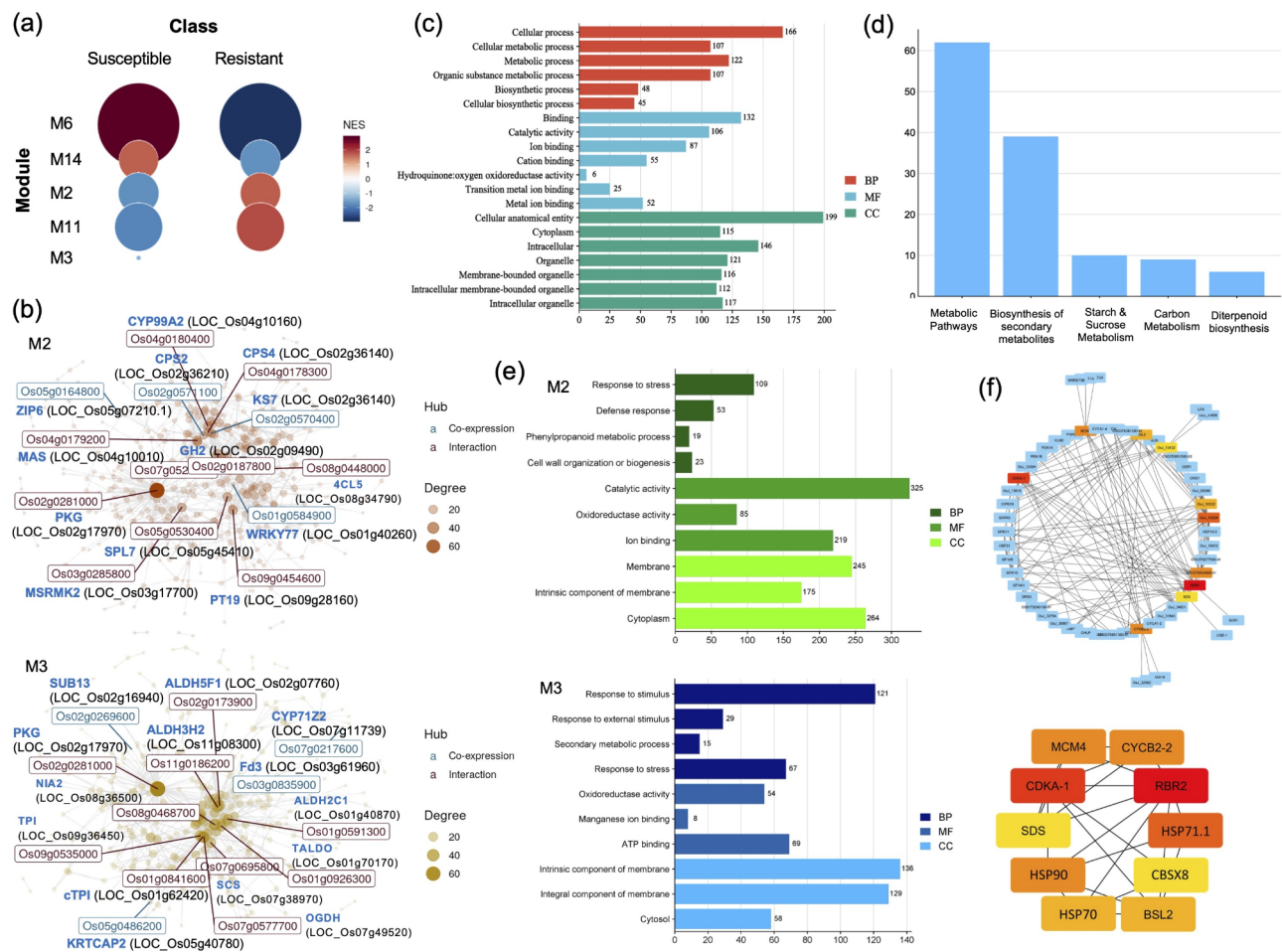


Fig. 5. Identification of important gene modules under blast pathogen treatment via mGCE analysis: **(a)** GSEA depicts module activity across susceptible and resistant class, generated using CEMiTool v1.30.0. The blue circle represents the downregulated gene module, and the red circle denotes the upregulated gene module; **(b)** mGCE-based PPI networks for modules M2 and M3. The top 10 genes are labelled and color-coded based on their origin: blue for genes from the CEMiTool module and red for those from the STRING interactions file. Node size corresponds to the degree of interactions; **(c)** GO enrichment analysis for hub genes across all modules; **(d)** Bar graph demonstrates enriched KEGG pathways involving hub genes; **(e)** ORA of modules M2 and M3; and **(f)** PPI network demonstrates 143 hub genes identified from all modules, with the top 10 subsequently determined using the MCC algorithm.

metabolism (*HSP71.1*, *HSP90*, *HSP70*, and *SDS2*) and genetic information processing (*PP2C* and *CYCB2;1*). *PP2C* was found to be involved in the MAPK signalling pathway and plant hormone signal transduction, whereas *RPS5* and *HSP90* in plant-pathogen interaction (Fig. 6c). The pathways in which these hub genes participated were also observed in various metabolic processes, including biosynthesis of secondary metabolites, metabolic pathways, diterpenoid biosynthesis, starch and sucrose metabolism, seleno compounds, benzoxazinoid biosynthesis, and carbon metabolism. In addition, modules in the blast pathogen were highly involved in metabolism and the genetic information system, with *HSP90*, *HSP70*, *MCM*, *PKG*, and *RPS5* for each category. Furthermore, the validation of the hub genes within the pathway maps was confirmed through integration with protein-protein interaction data (Fig. 6d).

Validation of *RPS5*, *PKG*, *HSP90*, *HSP70*, and *MCM* gene expressions using RT-qPCR

A comprehensive analysis was conducted for a deeper understanding of stress-induced transcriptional changes over time. A global gene expression study on susceptible plant MR219 exhibited significant vulnerability to environmental stress factors such as drought, salinity, and submergence. RT-qPCR showed diverse expressions under specific stress conditions and times. Table 3 lists qPCR validation primers, while Fig. 7 illustrates *RPS5*, *PKG*, *HSP90*, *HSP70*, and *MCM* gene expressions. In drought stress, the *RPS5* gene showed the maximum stress effects after 4 days by 12-fold changes from the initial treatment (Fig. 7a). A significant ninefold change was observed in the early 24 h, with a fivefold decrease in the next 48 h. In the blast pathogen infection, the *RPS5* gene revealed an increasing expression pattern of approximately 2 to sevenfold changes (Fig. 7b). Conversely, the expression level of the *PKG* gene decreases throughout the treatment from twelve to ninefold changes but

Condition	Total hub genes	Top 10 hub (RAP ID)	Top 10 hub (MSU ID)	Gene ID	Gene name	Chr
Drought	85	Os03g0835400	LOC_Os03g61920	<i>ETF A</i>	Electron transfer flavoprotein subunit alpha	3
		Os11g0482000	LOC_Os11g29190	<i>RPS5</i>	Resistance to <i>pseudomonas syringae</i> 5	11
		Os12g0618600	LOC_Os12g42400	<i>OsHAP2F</i>	Homeodomain-leucine zipper class 2 transcription factor F	12
		Os10g0467600	LOC_Os10g32970	<i>EIF504</i>	Eukaryotic translation initiation factor 4E isoform	10
		Os05g0333200	LOC_Os05g26890	<i>D1</i>	Daikoku dwarf	5
		Os09g0297400	LOC_Os09g12600	<i>PPT1</i>	Polypentenyltransferase 1	9
		Os06g0716700	LOC_Os06g50300	<i>HSP90</i>	Heat-shock protein 90	6
		Os04g0462500	LOC_Os04g38870	<i>GFI4B</i>	G-box factor 14-3-3b protein	4
		Os03g0200800	LOC_Os03g10370	<i>ARL1A</i>	ARF-like protein 1a	3
		Os02g0580300	LOC_Os02g36974	<i>GFI4E</i>	Gibberellin-insensitive dwarf protein 2	2
Salinity	106	Os03g0168100	LOC_Os03g07180	<i>LEA16</i>	Late embryogenesis abundant protein 16	3
		Os03g0322900	LOC_Os03g20680	<i>LEA17</i>	Late embryogenesis abundant protein 17	3
		Os06g0218500	LOC_Os06g11500	<i>MCM2</i>	Mini-chromosome maintenance protein 2	6
		Os12g0124700	LOC_Os12g03130	<i>CDC45-1</i>	Cell division control 45-1	12
		Os06g0520600	LOC_Os06g32860	<i>C3H43</i>	Zinc finger CCCH domain-containing protein 43	6
		Os03g0276800	LOC_Os03g16880	<i>HSP70</i>	Heat shock protein 70	3
		Os02g0281000	LOC_Os02g17970	<i>PKG</i>	Protein phosphatase 23	2
		Os03g0765000	LOC_Os03g55620	<i>Aurora-B</i>	Serine/threonine-protein kinase 12	3
		Os10g0505900	LOC_Os10g36180	Os10g0505900	Conserved hypothetical protein	10
		Os01g0885000	LOC_Os01g66180	<i>CYT C</i>	Cytochrome c	1
Tungro virus	253	Os05g0314100	LOC_Os05g24970	<i>SNU13</i>	Small nuclear ribonucleoprotein 13	5
		Os02g0324500	LOC_Os02g21900	<i>RPS7</i>	Ribosomal protein S7	2
		Os02g0489400	LOC_Os02g28810	<i>RPS8</i>	Ribosomal protein S8	2
		Os10g0466200	LOC_Os10g32870	<i>RPL11</i>	Ribosomal protein L11	10
		Os07g0434700	LOC_Os07g25410	<i>M24</i>	Peptidase M24	7
		Os03g0265400	LOC_Os03g15870	<i>RPL4</i>	Ribosomal protein L4	3
		Os02g0198900	LOC_Os02g10540	<i>RPL12</i>	Ribosomal protein L12	2
		Os11g0482000	LOC_Os11g29190	<i>RPS5</i>	Ribosomal protein S5	11
		Os02g0281000	LOC_Os02g17970	<i>PKG</i>	Protein phosphatase 23	2
		Os03g0241200	LOC_Os03g13800	<i>NHP2</i>	NHP2-like protein 1 (High mobility group-like nuclear protein 2 homolog 1)	3
Blast pathogen	143	Os01g0544450	LOC_Os01g36390	<i>MCM4</i>	Mini-chromosome maintenance protein 4	1
		Os03g0118400	LOC_Os03g02680	<i>CDKA-1</i>	Cyclin-dependent kinase A1	3
		Os03g0225200	LOC_Os03g12414	<i>SDS</i>	SPL11 cell-death suppressor	3
		Os06g0716700	LOC_Os06g50300	<i>HSP90</i>	Heat-shock protein 90	6
		Os03g0276800	LOC_Os03g16880	<i>HSP70</i>	Heat-shock protein 70	3
		Os12g0617900	LOC_Os12g42310	<i>BSL2</i>	Botrytis susceptibility 2	12
		Os08g0529200	LOC_Os08g41740	<i>CBSX8</i>	Cystathionine beta-synthase	8
		Os03g0276500	LOC_Os03g16860	<i>HSP71.1</i>	71.1 kda class I heat shock protein	3
		Os08g0538700	LOC_Os08g42600	<i>RBR2</i>	Retinoblastoma-related protein-2	8
		Os06g0726800	LOC_Os06g51110	<i>CYCB2-2</i>	Cyclin-B2-2 G2/mitotic-specific cyclin-B2-2	6

Table 1. List of key hub genes identified in response to drought, salinity, tungro virus, and blast pathogen conditions.

increases from six to tenfold changes under salinity treatment (Fig. 7c,d). For *HSP70*, the expression level decreases but later increases by 1- to fourfold after 1 month of tungro virus infection (Fig. 7e,f). Meanwhile, drought stress induced a significant increase in *HSP90* expression during the first 12 h of infection, reaching a ninefold change, followed by a gradual decrease to a twofold change after 48 h (Fig. 7g). However, *HSP90* levels remained largely unchanged in both control and stressed plants during the first 10 days of infection but showed a substantial increase, reaching an 18-fold change after 1 month of infection (Fig. 7h). During the tungro virus infection, the expression of the *MCM* gene showed a threefold increase after 1 month of infection compared to 10 days (Fig. 7i). Under 120 mM salinity treatment, *MCM* expression increased by fourfold after 5 days in the susceptible rice variety MR219 (Fig. 7j).

	Genes	MCC	DMNC	MNC	Degree	EPC	BottleNeck	EcCentricity	Closeness	Radiality	Betweenness	Stress	Clustering coefficient
Drought	RPS5	8	0.2842	4	6	20.464	12	0.14952	24.55	8.24184	603.8777	1966	0.26667
	HSP90	10	0.37893	4	6	19.559	3	0.12793	21.23571	7.60435	180.4277	560	0.26667
Salinity	MCM2	118	0.3321	13	13	26.426	4	0.2	36.73333	4.48101	339.2213	2234	0.33333
	HSP70	128	0.4242	11	13	28.367	3	0.25	41.91667	4.89873	479.0411	2216	0.33333
	PKG	259	0.21551	29	42	31.591	73	0.33333	58	5.43038	3887.438	10,722	0.07666
Tungro Virus	HSP90	330	0.43064	15	15	72.377	8	0.15173	68.51667	7.80933	613.931	5244	0.40952
	HSP70	90	0.27027	14	14	72.265	2	0.13005	69.81243	7.852	1065.666	692	0.26374
	MCM4	5189	0.46832	12	15	71.116	12	0.13005	67.13095	7.68131	2934.596	15,690	0.30476
Blast Pathogen	RPS5	1.13E+09	0.91799	19	20	54.418	2	0.2	61.18333	5.51563	189.8189	1626	0.72105
	PKG	1.13E+09	0.65654	26	26	57.456	1	0.2	67.36667	5.76563	437.4791	4920	0.51385

Table 2. The list of hub genes detected as the hubs in both abiotic and biotic stresses.

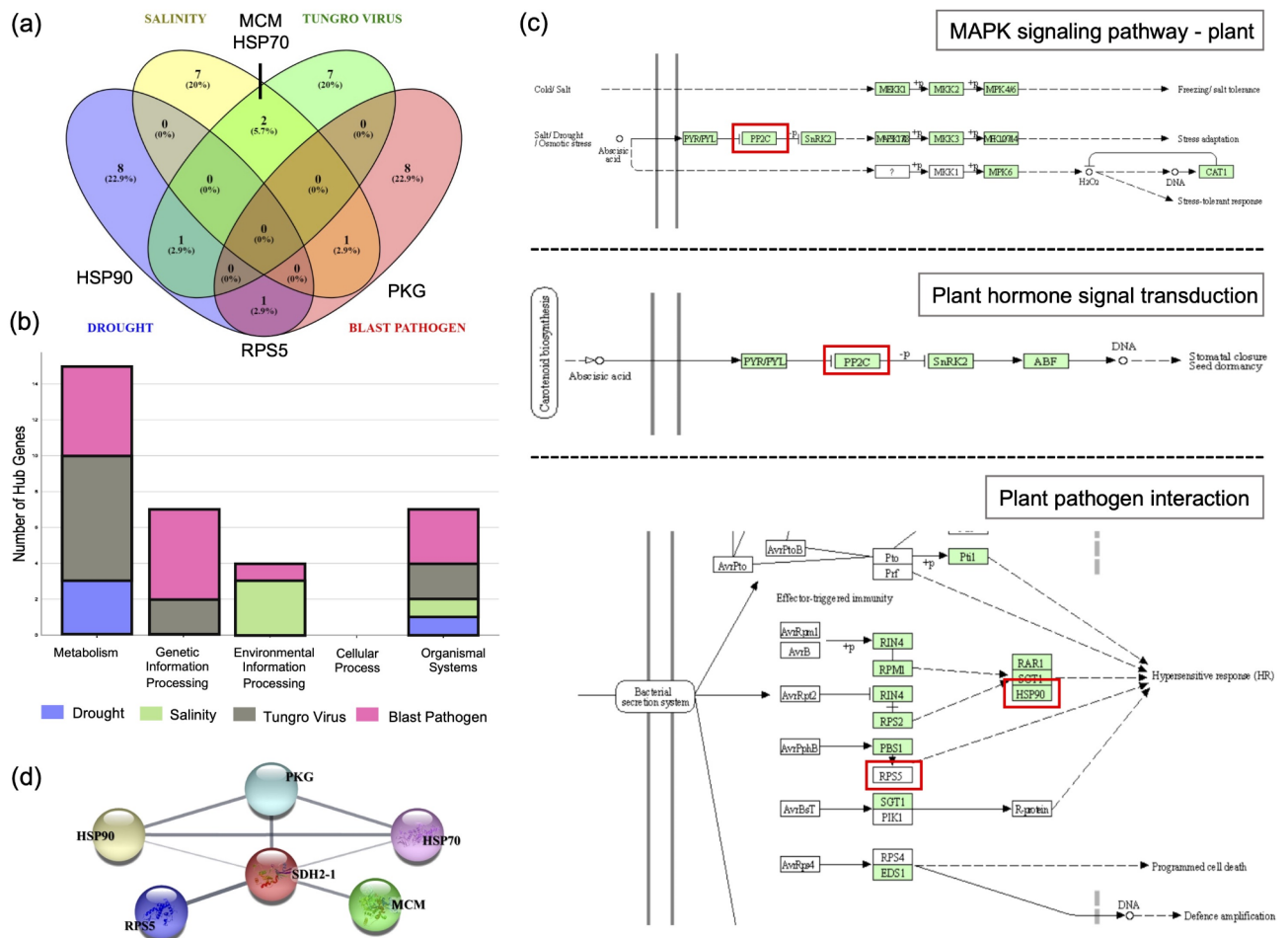


Fig. 6. (a) Venn diagram of each dataset for drought, salinity, tungro virus and blast pathogen being overlapped to find the overlapped hub genes; (b) Critical genes in modular networks linked to different stressors categorised into primary pathways: cellular processes, environmental information processing, genetic information processing, and organismal systems; (c) The selected hub genes, highlighted in the red box, were mapped in KEGG pathways using KEGG Mapper; (d) The network showed SDH2-1 as mediator for five hub genes (*HSP90*, *HSP70*, *PKG*, *RPS5*, and *MCM*).

Discussion

The main purpose of this study is to identify and validate the hub genes involved in salinity, drought, and infection by tungro and blast to understand the potential combined stress mechanisms. In this study, 587 hub genes (all mGCEs), of which 35 were the top hub genes, were detected in all conditions. Among the 35 hub genes, 5 genes, namely *RPS5*, *PKG*, *HSP90*, *HSP70*, and *MCM*, were present in both biotic and abiotic stress.

Gene	Gene ID	Forward primer (F)	Reverse primer (R)	Annealing temperature (°C)	Amplicon size (bp)	GC Content F (%)	GC Content R (%)
PKG	Os02g0281000	AGAGATGTACAGTTTGGGGCA	CACAGGATTAGCACACACACCG	61.2	116	47.62	54.55
MCM2	Os01g0544450	GATAATTCGGTGCAGCTCGG	CAGATGTCGGCTAGCTGAAC	61.2	113	55	55
HSP90	Os06g0716700	AGTCCTTGCCGAGTTTGAGA	CAAGGATAACACCCGCTCG	61.2	103	50	57.89
HSP70	Os03g0277300	CAAGGATAACACCCGCTCGC	GACACGTTTCATGATGCCGTT	60.2	117	60	50
RPS5	Os11g0482000	ACCAACTCCCTCATGATGCA	GGCATCTACGATGACCTGGA	59.2	109	50	55
U6	Os05g0389300	TACAGATAAGATTAGCATGGCCC	GGACCATTTCTCGATTGTGACG	58.0	103	43.48	50.0

Table 3. Primers used in this study for qPCR validation.

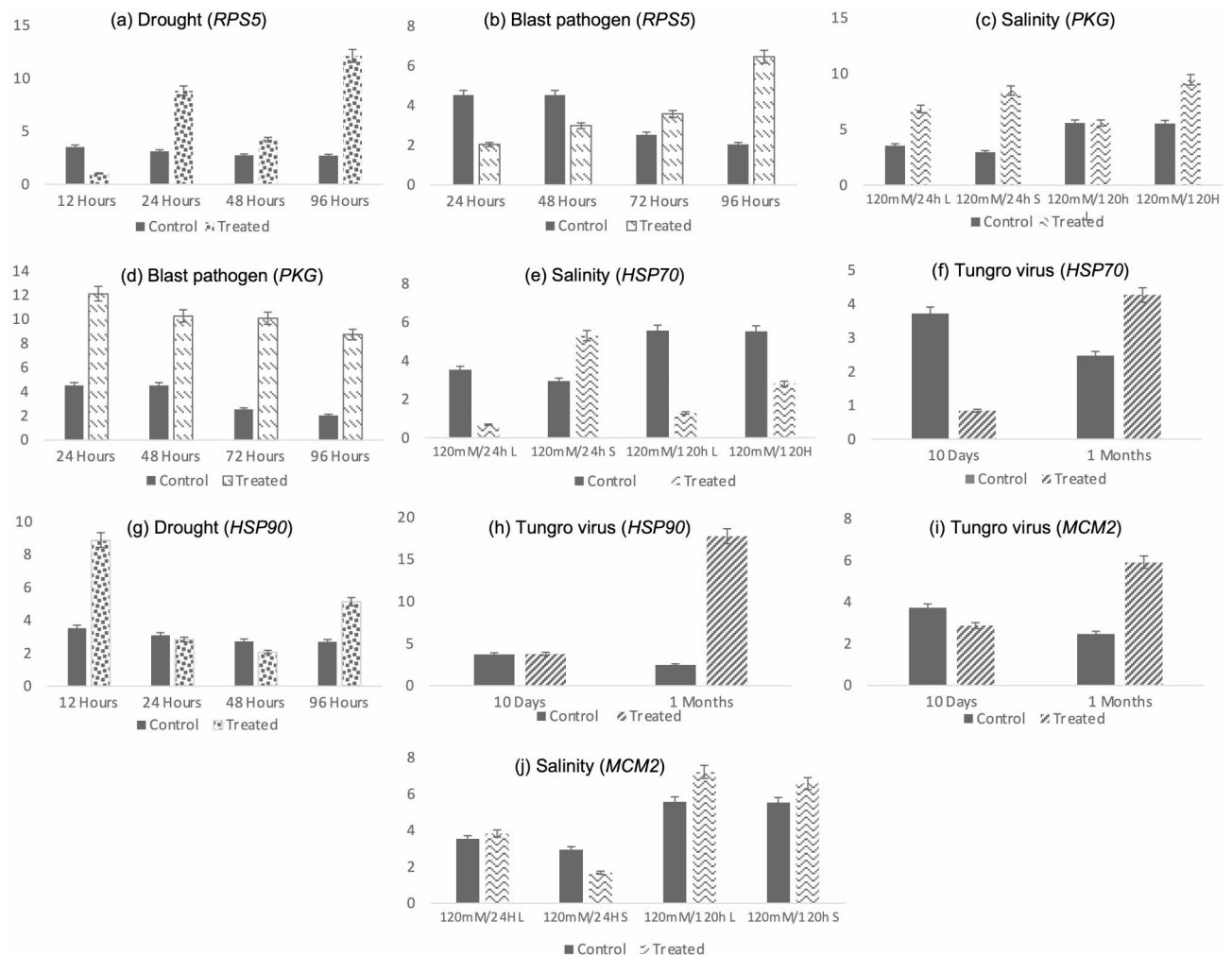


Fig. 7. RT-qPCR validations on five co-expressed hub genes among the four stresses: drought, salinity, tungro virus and blast pathogen. The bar chart illustrates the average value and the standard error for three sets of biological replicates and three sets of technical replicates. The variation in gene expression between the control (WT) and each stress with different time points was evaluated using a one-way ANOVA approach, with a significance threshold set at a p-value less than 0.05. The error bars on the chart represents the standard error.

ORA revealed that mGCE in drought, tungro, and blast datasets were significantly enriched in response to water deprivation, salt stress, ABA stimulus, and signalling. The salinity group, on the other hand, were predicted to be involved in the response to biotic stimulus and fungus, defence response, and terpenoid metabolic process.

The ORA findings indicated that water deprivation-responsive genes appeared to be activated in drought. Prior studies have demonstrated that during drought, the transport of ions and water across membranes plays a critical role in regulating turgor pressure fluctuations within guard cells, ultimately resulting in stomatal closure⁴⁴. Drought can also diminish leaf water potential, leading to the inhibition of stomatal opening. Consequently, the

impact of ABA on ion transport systems can alter stomatal responses, thereby impacting the capacity of plants to withstand water stress⁴⁵. Additionally, it has also been revealed that ABA responds to salinity stress. Huang et al.⁴⁶ reported that salt stress induces the accumulation of ABA in primary roots, which suppresses cell division and stimulates growth in cortical cells within the root meristem, leading to shorter, thicker primary roots that may swell. Salinity has detrimental effects on plants through two primary mechanisms⁴⁶. Firstly, elevated soil salt levels decrease porosity and hydraulic permeability, which, in turn, reduces water potential, leading to water stress and subsequent physiological drought. Secondly, ions such as sodium (Na^+) damage cell membranes and proteins, causing their destabilisation⁴⁷.

In the tungro virus, manganese ion (Mn^{2+}) binding and abiotic stimulus response are upregulated among the modular genes. Given that, Mn^{2+} serves as essential plant micronutrients in photosynthesis, enzyme activation, and antioxidant defence⁴⁸, and their deficiency can impede crop yields and increase crop susceptibility to pathogen infections⁴⁹. In a study on tomatoes by Heine et al., Mn^{2+} was demonstrated as an essential component of the plant's defence system⁴⁹. Mn substantially reduced black leaf mould without inhibiting growth or production. In addition, Mn^{2+} is known to activate or trigger phytoalexins, which are chemical compounds that assist plants in responding to and recovering from pathogen attacks⁵⁰. This study demonstrates that root development and defence response against fungus are also vital processes during blast pathogen infection. The strong connections between the functions of plant roots and blast pathogens underscore the strategic importance of plant root systems in defending against pathogenic threats⁵¹. During a pathogen attack, root growth and root-associated microorganisms are essential in establishing plant systemic resistance⁵². Apart from root development, rice also developed resistance against *M. oryzae* and defence against fungi during infection⁴⁸. In response to external stimuli, MAPK relays signal from the cell membrane to the nucleus, functioning as a defence mechanism against *M. oryzae*. Therefore, the module detection has unveiled novel insights into the molecular disturbances caused by abiotic and biotic stress. These findings may help define the genes that drive the responses to various stresses, thus offering potential solutions for effective crop protection.

Furthermore, this finding identified five essential hub genes, i.e., *RPS5*, *PKG*, *HSP90*, *HSP70*, and *MCM*. *RPS5* is essential for protein synthesis and has several functions in plant growth and development, photosynthesis, and enhanced stress tolerance in Arabidopsis. A mutant of the *rps5* gene showed impairment in both photosystem I and II⁵³, increased resistance to drought and salinity stress^{54,55} and was shown to be susceptible to bacterial infections⁵⁶. The *RP* genes respond differently to environmental stimuli, including abiotic and biotic impacts. These variables have a direct influence on plant development, the transcriptional regulation of *RP* genes, and, as a result, the ribosome biogenesis process⁵⁷. Aside from their role as translational machinery, these proteins can also function as stress signalling pathways⁵⁸. In recent years, there have been documented cases of ribosomal proteins exhibiting functions related to disease resistance and responses to stress⁵⁹. Apart from that, the amounts of ribosomal proteins, protein chaperones, and proteases changed noticeably. These proteins perform critical functions in protein synthesis and modification, contributing to stress adaptation. Pan et al. (2018)⁶⁰ reported that drought dramatically boosted some of the ribosomal proteins. A study by Moin et al. (2021)⁶¹ concluded that the *RPS5* gene was upregulated in the resistant genotype towards fungal blast disease in rice. Hence, *RPS5* might actively participate in defence-related signalling pathways or play a role in the fundamental metabolic mechanisms contributing to pest resistance. This involvement could manifest as heightened overall photosynthesis and enhanced vigour of the plant during stressful conditions. During an invasion, pathogens invade plant host cells by precisely targeting and inhibiting specific plant immune receptors, with the *RPS5* gene acting as a receptor that recognises and binds to the pathogen effectors⁶².

PKG plays a multifaceted role, including coping with stress, initiating seed germination, stimulating the production of α -amylase, regulating the movement of stomata, guiding the reorientation of pollen tubes and cell polarity, and facilitating the production of anthocyanins and flavonoids⁶³. This study showed that *PKG* is vital in the initial infection phase of the blast pathogen (12 h) and displayed an increasing trend in expression during salinity exposure, from 120 mM/24 h to 120 mM/120 h. Conclusive evidence highlights the role of *PKG* as a mediator of biophysical signal molecules and its function as a messenger when exposed to stress by converting signals and initiating subsequent reactions within the cellular environment⁶⁴. A study by Shen et al.⁶⁴ found that the lack of the *PKG* gene can lead to growth stagnation with reduced shoot and root length. Moreover, the *pkg* mutant produced more reactive oxygen species under salinity conditions and higher ROS levels.

Regarding the blast pathogen response, an eightfold increase was observed in the expression of the *PKG* gene compared to the control during the initial 24-h treatment. Protein kinase G, also known as cyclic guanosine 3',5'-monophosphate (cGMP), can regulate the defence gene expression⁶⁵. Previous research has shown that cGMP exists in plants and may trigger defensive gene expression in tobacco, indicating its significant role in plant defence responses^{66–68}. The study by Hussain et al.⁶⁹ on genetically modified GC plants revealed over 50-fold accumulation of cGMP compared to normal levels, typical cell death, and increased resistance when induced by avirulent pathogens. However, the study of cGMP's detailed role in plant defence responses is arduous because the enzymes involved in its synthesis and degradation are currently unidentified.

Other hub genes that were co-expressed during the stress response included the *HSP70* and *HSP90* genes. The *HSP70* gene, belonging to a highly conserved group of chaperones that play essential roles in various cellular processes, has significantly modulated stress responses in host plants^{70,71}. The RT-qPCR analysis showed that the *HSP70* gene had the highest expression during salinity stress in the leaf and showed an increasing pattern over infection periods with the tungro virus. This observation supports the notion that when subjected to stressors, plants respond by upregulating the production of the *HSP70* gene, which in turn protects cellular components, prevents damage, and maintains cellular homeostasis⁷². The *HSP70* gene was also discovered to be upregulated in response to abiotic and plant-pathogen interactions, suggesting that the interaction involving the *HSP70* gene could have positive and negative regulatory effects on viral infections and environmental stresses⁷³.

HSP90, on the other hand, mirrors the function of *HSP70*, which also plays essential roles in both abiotic and biotic stress⁷⁴. During high temperatures, many HSPs were triggered and accumulated a large amount of heat shock response to maintain cellular stability⁷⁵. It has been reported that the *OsHSP90* positively regulates drought stress tolerance by influencing the balance of ROS and facilitating osmotic adjustment⁷⁶. In this study, notable changes in *OsHSP90* were discovered, i.e., the 12-fold change in tungro virus compared to a fivefold change under drought stress conditions. Lu et al.⁷⁷ reported that the *HSP90* gene plays a crucial role in enhancing plant resistance to the potato virus X and tobacco mosaic virus. This finding supports a similar discovery by Zhang et al.⁷⁸, which demonstrated that the *HSP90* gene exhibited comparable tolerance under both biotic and abiotic stress in cucumbers.

This study also predicted *MCM* as a critical gene in biotic and abiotic stress. *MCM* is a replicative helicase that serves as a licensing factor in DNA replication, ensuring the precise duplication of genomic DNA during the S phase of a single cell cycle⁷⁹. The discovery of six *MCM* coding genes reveals that the *MCM2-7* genes are co-ordinately regulated throughout the developmental process in higher plants⁸⁰. In this current study, *MCM2* and *MCM4* genes exhibited high expression during salinity and tungro virus stresses. It was reported that the overexpression of *MCM* can create a tolerance to salt stress without yield loss⁸¹. Interestingly, it was found that the interaction between plant hormones and plant helicase can create chemical compounds functioning as signalling molecules, prompting plants to adapt and thrive in diverse stressful environments⁸². *MCM* gene, also known as the environmental stress response gene, is associated with the plant hormones auxin and abscisic acid.

Interestingly, this study discovered that the complex II iron-sulphur subunit of succinate dehydrogenase (*SDH2-1*) serves as a mediator connecting all the hub genes, including *RPS5*, *PKG*, *HSP90*, *HSP70*, and *MCM*. *SDH* has a central position in mitochondrial metabolism, serving as the sole enzyme in both the tricarboxylic acid (TCA) cycle and the electron transport chain⁸³. A mutation in the *sdh* gene can lead to changes in photosynthesis, stomata function, root elongation, and defence against fungi⁸⁴. In addition, *SDH2* plays a role in influencing stomatal opening, the plant defence response, and stress responses that depend on ROS⁸⁵. Dysfunctional *SDH* can result in alterations in tissue-specific respiration rates and changes in the production of ROS within the mitochondria⁸⁵. Mitochondrial ROS (mtROS) plays a pivotal role in plant responses to stress and pathogens. Various stressors, including drought, high light intensity, heat, and pathogen attack, can lead to mitochondrial dysfunction and the subsequent production of mtROS⁸⁵. Hence, the role of *SDH* may need extensive assessment in a PPI study to gain insights into the regulatory mechanisms and interactions that underlie the complex interplay of hub genes in combined stress.

Conclusion

In conclusion, the mGCE analysis provides an in-depth examination of essential hub genes potentially involved in plant responses against biotic and abiotic stresses. Several mGCEs play an important role in abiotic and biotic stress by activating reactions related to water deprivation, root development, defence against fungi, and biotic stimuli. Of 35 hub genes, 5 genes—*RPS5*, *PKG*, *HSP90*, *HSP70*, and *MCM*—are involved in both biotic and abiotic treatments, suggesting their critical roles as prominent regulators for combined stresses in rice. While the results have certain limitations, additional experimental studies are necessary to confirm their response to combined stresses, providing a reliable basis for further research into the molecular mechanisms. The findings provide valuable insights that can enhance plant stress diagnosis, improve traits, and contribute to the development of better management strategies for stress-related issues.

Data availability

The downloaded raw and normalised microarray data are publicly available under the NCBI GEO database with the accession numbers GSE30449, GSE79043, GSE16142, and GSE62422.

Received: 24 September 2024; Accepted: 4 March 2025

Published online: 12 March 2025

References

1. Firdaus, R. B. R., Leong Tan, M., Rahmat, S. R. & Senevi Gunaratne, M. Paddy, rice and food security in Malaysia: A review of climate change impacts. *Cogent. Soc. Sci.* **6**, 1818373 (2020).
2. Arora, N. K. Impact of climate change on agriculture production and its sustainable solutions. *Environ. Sustain.* **2**, 95–96 (2019).
3. Pandey, P., Irulappan, V., Bagavathiannan, M. V. & Senthil-Kumar, M. Impact of combined abiotic and biotic stresses on plant growth and avenues for crop improvement by exploiting physio-morphological traits. *Front. Plant Sci.* **8**, 537 (2017).
4. Bitu, C. E. & Gerats, T. Plant tolerance to high temperature in a changing environment: Scientific fundamentals and production of heat stress-tolerant crops. *Front. Plant Sci.* **4**, 273 (2013).
5. Velásquez, A. C., Castroverde, C. D. M. & He, S. Y. Plant-pathogen warfare under changing climate conditions. *Curr. Biol.* **28**, R619–R634 (2018).
6. Afroz, R., Muhibbullah, M. & Morshed, M. N. Factors affecting the intention of the rice farmers to adopt the integrated cash Waqf environmental protection model: An empirical study in Kedah Malaysia. *J. Asian Finance Econ. Bus.* **6**, 189–199 (2019).
7. Minh, L. T. et al. Effects of salinity stress on growth and phenolics of rice (*Oryza sativa* L.). *Int. Lett. Nat. Sci.* **57**, 1–10 (2016).
8. Samsuddin Sah, S., Maulud, K. N. A., Sharil, S., Karim, O. A. & Nahar, N. F. A. Impact of saltwater intrusion on paddy growth in Kuala Kedah, Malaysia. *J. Sustain. Sci. Manag.* **16**, 15–30 (2021).
9. Kannan, M., Saad, M. M., Talip, N., Baharum, S. N. & Bunawan, H. Complete genome sequence of rice *Tungro bacilliform* virus infecting Asian rice (*Oryza sativa*) in Malaysia. *Microbiol. Resour. Announc.* **8**, e00262–e00319 (2019).
10. Faizal Azizi, M. M. & Lau, H. Y. Advanced diagnostic approaches developed for the global menace of rice diseases: A review. *Can. J. Plant Pathol.* **44**, 627–651 (2022).
11. Kulkarni, K. & Peshwe, S. Screening, isolation and molecular identification of rice pathogen *Magnaporthe oryzae*. *Int. J. Adv. Res.* **7**, 428–433 (2019).

12. Singh, B. K. et al. Climate change impacts on plant pathogens, food security and paths forward. *Nat. Rev. Microbiol.* **21**, 640–656 (2023).
13. Porter, J. R. & Semenov, M. A. Crop responses to climatic variation. *Philos. Trans. R. Soc. Lond. B. Biol. Sci.* **360**, 2021–2035 (2005).
14. Jäkel, S. & Williams, A. What have advances in transcriptomic technologies taught us about human white matter pathologies?. *Front. Cell Neurosci.* **14**, 238 (2020).
15. Altaf-Ul-Amin, M., Afendi, F. M., Kiboi, S. K. & Kanaya, S. Systems biology in the context of big data and networks. *Biomed. Res. Int.* **2014**, 428570 (2014).
16. Langfelder, P., Mischel, P. S. & Horvath, S. When is hub gene selection better than standard meta-analysis?. *PLoS One* **8**, e61505 (2013).
17. Ma, S., Bohnert, H. J. & Dinesh-Kumar, S. P. AtGGM2014, an Arabidopsis gene co-expression network for functional studies. *Sci. China Life Sci.* **58**, 276–286 (2015).
18. Abdullah-Zawawi, M.-R., Tan, L.-W., Ab Rahman, Z., Ismail, I. & Zainal, Z. An integration of transcriptomic data and modular gene co-expression network analysis uncovers drought stress-related hub genes in transgenic rice overexpressing OsAbp57. *Agronomy* **12**, 1959 (2022).
19. Ramkumar, M. K. et al. Identification of major candidate genes for multiple abiotic stress tolerance at seedling stage by network analysis and their validation by expression profiling in rice (*Oryza sativa* L.). *3 Biotech* **12**, 127 (2022).
20. Zhang, Y. et al. Rice co-expression network analysis identifies gene modules associated with agronomic traits. *Plant Physiol.* **190**, 1526–1542 (2022).
21. Zeng, Z., Zhang, S., Li, W., Chen, B. & Li, W. Gene-coexpression network analysis identifies specific modules and hub genes related to cold stress in rice. *BMC Genomics* **23**, 251 (2022).
22. Sharma, N., Madan, B., Khan, M. S., Sandhu, K. S. & Raghuram, N. Weighted gene co-expression network analysis of nitrogen (N)-responsive genes and the putative role of G-quadruplexes in N use efficiency (NUE) in rice. *Front. Plant Sci.* **14**, 1135675 (2023).
23. Azad, M., Tohidfar, M., Ghanbari Moheb Seraj, R., Mehralian, M. & Esmaeilzadeh-Salestani, K. Identification of responsive genes to multiple abiotic stresses in rice (*Oryza sativa*): A meta-analysis of transcriptomics data. *Sci. Rep.* **14**, 5463 (2024).
24. Russo, P. S. T. et al. CEMiTool: A bioconductor package for performing comprehensive modular co-expression analyses. *BMC Bioinform.* **19**, 56 (2018).
25. Cheng, C. W., Beech, D. J. & Wheatcroft, S. B. Advantages of CEMiTool for gene co-expression analysis of RNA-seq data. *Comput. Biol. Med.* **125**, 103975 (2020).
26. Barrett, T. et al. NCBI GEO: Archive for functional genomics data sets - Update. *Nucleic Acids Res.* **41**, D991–D995 (2013).
27. Moumeni, A. et al. Comparative analysis of root transcriptome profiles of two pairs of drought-tolerant and susceptible rice near-isogenic lines under different drought stress. *BMC Plant Biol.* **11**, 174 (2011).
28. Hossain, M. R., Bassel, G. W., Pritchard, J., Sharma, G. P. & Ford-Lloyd, B. V. Trait specific expression profiling of salt stress responsive genes in diverse rice genotypes as determined by modified significance analysis of microarrays. *Front. Plant Sci.* **7**, 567 (2016).
29. Lee, J.-H. et al. Single nucleotide polymorphisms in a gene for translation initiation factor (eIF4G) of rice (*Oryza sativa*) associated with resistance to Rice tungro spherical virus. *Mol. Plant Microbe Interact.* **23**, 29–38 (2010).
30. Tanabe, S. et al. Spatial regulation of defense-related genes revealed by expression analysis using dissected tissues of rice leaves inoculated with *Magnaporthe oryzae*. *J. Plant Physiol. Pathol.* **2** (2014).
31. Korotkevich, G., Sukhov, V., Budin, N., Shpak, B., Artyomov, M. N. & Sergushichev, A. Fast gene set enrichment analysis. *BioRxiv*, 060012 (2016).
32. Wu, T. et al. clusterProfiler 4.0: A universal enrichment tool for interpreting omics data. *Innovation (Cambridge (Mass.))* **2**, 100141 (2021).
33. Goodstein, D. M. et al. Phytozome: A comparative platform for green plant genomics. *Nucleic Acids Res.* **40**, D1178–D1186 (2012).
34. Kurata, N. & Yamazaki, Y. Oryzabase. An integrated biological and genome information database for rice. *Plant Physiol.* **140**, 12–17 (2006).
35. Young, M. D., Wakefield, M. J., Smyth, G. K. & Oshlack, A. Gene ontology analysis for RNA-seq: Accounting for selection bias. *Genome Biol.* **11**, R14 (2010).
36. Kanehisa, M., Sato, Y. & Kawashima, M. KEGG mapping tools for uncovering hidden features in biological data. *Protein Sci.* **31**, 47–53 (2022).
37. Szklarczyk, D. et al. STRING v11: protein–protein association networks with increased coverage, supporting functional discovery in genome-wide experimental datasets. *Nucleic Acids Res.* **47**, D607–D613 (2019).
38. Doncheva, N. T., Morris, J. H., Gorodkin, J. & Jensen, L. J. Cytoscape StringApp: Network analysis and visualization of proteomics data. *J. Proteome Res.* **18**, 623–632 (2019).
39. Chin, C. H. et al. cytoHubba: Identifying hub objects and sub-networks from complex interactome. *BMC Syst. Biol.* **8**, S11 (2014).
40. Clough, E. et al. NCBI GEO: Archive for gene expression and epigenomics data sets: 23-year update. *Nucleic Acids Res.* **52**, D138–D144 (2024).
41. Metsalu, T. & Vilo, J. ClustVis: a web tool for visualizing clustering of multivariate data using principal component analysis and heatmap. *Nucleic Acids Res.* **43**, W566–W570 (2015).
42. Hayashi, N., Kobayashi, N., Vera Cruz, C. M. & Fukuta, Y. Protocols for the sampling of diseased specimens and evaluation of blast disease in rice. *JIRCAS Working Report* **63**, 17–33 (2009).
43. Pfaffl, M. W., Horgan, G. W. & Dempfle, L. Relative expression software tool (REST) for group-wise comparison and statistical analysis of relative expression results in real-time PCR. *Nucleic Acids Res.* **30**, e36 (2002).
44. Osakabe, Y., Osakabe, K., Shinozaki, K. & Tran, L.-S.P. Response of plants to water stress. *Front. Plant Sci.* **5**, 86 (2014).
45. Slawinski, L. et al. Responsiveness of early response to dehydration six-like transporter genes to water deficit in *Arabidopsis thaliana* leaves. *Front. Plant Sci.* **12**, 708876 (2021).
46. Huang, Y. et al. Salt stress promotes abscisic acid accumulation to affect cell proliferation and expansion of primary roots in rice. *Int. J. Mol. Sci.* **22**, 10892 (2021).
47. Hasanuzzaman, M. & Fujita, M. Plant responses and tolerance to salt stress: Physiological and molecular interventions. *Int. J. Mol. Sci.* **23**, 4810 (2022).
48. Chung, H. et al. Comparative pathogenicity and host ranges of *Magnaporthe oryzae* and related species. *Plant Pathol. J.* **36**, 305–313 (2020).
49. Heine, G. et al. Effect of manganese on the resistance of tomato to *Pseudocercospora fuligena*. *J. Plant Nutr. Soil Sci.* **174**, 827–836 (2011).
50. Tripathi, R. et al. Plant mineral nutrition and disease resistance: A significant linkage for sustainable crop protection. *Front. Plant Sci.* **13**, 883970 (2022).
51. Devanna, B. N. et al. Understanding the dynamics of blast resistance in rice-*Magnaporthe oryzae* interactions. *J. Fungi (Basel)* **8**, 584 (2022).
52. Zhu, L., Huang, J., Lu, X. & Zhou, C. Development of plant systemic resistance by beneficial rhizobacteria: Recognition, initiation, elicitation and regulation. *Front. Plant Sci.* **13**, 952397 (2022).
53. Zhang, J. et al. Plastid ribosomal protein S5 is involved in photosynthesis, plant development, and cold stress tolerance in *Arabidopsis*. *J. Exp. Bot.* **67**, 2731–2744 (2016).

54. Krieger-Liszka, A., Fufezan, C. & Trebst, A. Singlet oxygen production in photosystem II and related protection mechanism. *Photosynth. Res.* **98**, 551–564 (2008).
55. Moin, M., Bakshi, A., Madhav, M. S. & Kirti, P. B. Expression profiling of ribosomal protein gene family in dehydration stress responses and characterization of transgenic rice plants overexpressing RPL23A for water-use efficiency and tolerance to drought and salt stresses. *Front. Chem.* **5**, 97 (2017).
56. Till, C. J. et al. The *Arabidopsis thaliana* N-recognition E3 ligase PROTEOLYSIS1 influences the immune response. *Plant Direct* **3**, e00194 (2019).
57. Fromont-Racine, M., Senger, B., Saveanu, C. & Fasiolo, F. Ribosome assembly in eukaryotes. *Gene* **313**, 17–42 (2003).
58. Warner, J. R. & McIntosh, K. B. How common are extraribosomal functions of ribosomal proteins? *Mol. Cell* **34**, 3–11 (2009).
59. Nagaraj, S., Senthil-Kumar, M., Ramu, V. S., Wang, K. & Mysore, K. S. Plant ribosomal proteins, RPL12 and RPL19, play a role in nonhost disease resistance against bacterial pathogens. *Front. Plant Sci.* **6**, 1192 (2015).
60. Pan, J. et al. Comparative proteomic investigation of drought responses in foxtail millet. *BMC Plant Biol.* **18**, 315 (2018).
61. Moin, M. et al. Study on transcriptional responses and identification of ribosomal protein genes for potential resistance against brown planthopper and gall midge pests in rice. *Curr. Genomics* **22**, 98–110 (2021).
62. Yan, X. et al. The transcriptional landscape of plant infection by the rice blast fungus *Magnaporthe oryzae* reveals distinct families of temporally co-regulated and structurally conserved effectors. *Plant Cell* **35**, 1360–1385 (2023).
63. Isner, J.-C. & Maathuis, F. J. M. Measurement of cellular cGMP in plant cells and tissues using the endogenous fluorescent reporter FlnCG. *Plant J.* **65**, 329–334 (2011).
64. Shen, Q. et al. Dual activities of plant cGMP-dependent protein kinase and its roles in gibberellin signaling and salt stress. *Plant Cell* **31**, 3073–3091 (2019).
65. Lamotte, O., Courtois, C., Barnavon, L., Pugin, A. & Wendehenne, D. Nitric oxide in plants: The biosynthesis and cell signalling properties of a fascinating molecule. *Planta* **221**, 1–4 (2005).
66. Meier, S. et al. Deciphering cGMP signatures and cGMP-dependent pathways in plant defence. *Plant Signal Behav.* **4**, 307–309 (2009).
67. Wu, M. et al. Heme oxygenase-1 is involved in nitric oxide- and cGMP-induced α -Amy2/54 gene expression in GA-treated wheat aleurone layers. *Plant Mol. Biol.* **81**, 27–40 (2013).
68. Świeżawska, B., Jaworski, K., Duszyn, M., Pawelek, A. & Szmidi-Jaworska, A. The *Hippeastrum hybridum* PepR1 gene (HpPepR1) encodes a functional guanylyl cyclase and is involved in early response to fungal infection. *J. Plant Physiol.* **216**, 100–107 (2017).
69. Hussain, J. et al. Constitutive cyclic GMP accumulation in *Arabidopsis thaliana* compromises systemic acquired resistance induced by an avirulent pathogen by modulating local signals. *Sci. Rep.* **6**, 36423 (2016).
70. Al-Wahaibi, M. H. Plant heat-shock proteins: A mini review. *J. King Saud. Univ. Sci.* **23**, 139–150 (2011).
71. Aghaie, P. & Tafreshi, S. A. H. Central role of 70-kDa heat shock protein in adaptation of plants to drought stress. *Cell Stress Chaperones* **25**, 1071–1081 (2020).
72. Sarkar, N. K., Kundnani, P. & Grover, A. Functional analysis of Hsp70 superfamily proteins of rice (*Oryza sativa*). *Cell Stress Chaperones* **18**, 427–437 (2013).
73. Aparicio, F. et al. Virus induction of heat shock protein 70 reflects a general response to protein accumulation in the plant cytosol. *Plant Physiol.* **138**, 529–536 (2005).
74. Wang, L. et al. Genome structures and evolution analysis of Hsp90 gene family in *Brassica napus* reveal the possible roles of members in response to salt stress and the infection of *Sclerotinia sclerotiorum*. *Front. Plant Sci.* **13**, 854034 (2022).
75. Richter, K., Haslbeck, M. & Buchner, J. The heat shock response: Life on the verge of death. *Mol. Cell* **40**, 253–266 (2010).
76. Xiang, J. et al. Overexpressing heat-shock protein OsHSP50.2 improves drought tolerance in rice. *Plant Cell Rep.* **37**, 1585–1595 (2018).
77. Lu, R. et al. High throughput virus-induced gene silencing implicates heat shock protein 90 in plant disease resistance. *EMBO J.* **22**, 5690–5699 (2003).
78. Zhang, K. et al. Genome-wide characterization of HSP90 gene family in cucumber and their potential roles in response to abiotic and biotic stresses. *Front. Genet.* **12**, 584886 (2021).
79. Tuteja, N., Tran, N. Q., Dang, H. Q. & Tuteja, R. Plant MCM proteins: Role in DNA replication and beyond. *Plant Mol. Biol.* **77**, 537–545 (2011).
80. Herridge, R. P., Day, R. C. & Macknight, R. C. The role of the MCM2-7 helicase complex during *Arabidopsis* seed development. *Plant Mol. Biol.* **86**, 69–84 (2014).
81. Sarwat, M. & Tuteja, N. Ch. 7 DNA helicase-mediated abiotic stress tolerance in plants. In *Biochemical, Physiological and Molecular Avenues for Combating Abiotic Stress Tolerance in Plants* (ed. Wani, S. H.) 103–115 (Academic Press, 2018).
82. Mohapatra, M. D., Poosapati, S., Sahoo, R. K. & Swain, D. M. Helicase: A genetic tool for providing stress tolerance in plants. *Plant Stress* **9**, 100171 (2023).
83. Huang, S. & Millar, A. H. Succinate dehydrogenase: The complex roles of a simple enzyme. *Curr. Opin. Plant Biol.* **16**, 344–349 (2013).
84. Tivendale, N. D. et al. Knockdown of succinate dehydrogenase assembly factor 2 induces reactive oxygen species-mediated auxin hypersensitivity causing pH-dependent root elongation. *Plant Cell Physiol.* **62**, 1185–1198 (2021).
85. Huang, H., Ullah, F., Zhou, D.-X., Yi, M. & Zhao, Y. Mechanisms of ROS regulation of plant development and stress responses. *Front. Plant Sci.* **10**, 800 (2019).

Author contributions

Izreen Izzati Razalli: Formal analysis, Writing—original draft, Data curation, Investigation, Validation, Visualization. Muhammad-Redha Abdullah-Zawawi: Conceptualization, Methodology, Writing—original draft, Project administration, Data curation, Writing—review and editing, Visualization, Supervision. Rabiatal Adawiah Zainal Abidin: Conceptualization, Methodology, Data curation, Writing—review and editing, Supervision. Sarahani Harun: Data curation, Writing—review & editing. Muhamad Hafiz Che Othman: Writing—review and editing. Ismanizan Ismail: Writing—review and editing. Zamri Zainal: Conceptualization, Methodology, Data curation, Writing—review and editing, Funding acquisition, Project administration, Supervision.

Funding

This research was funded by Fundamental Research Grant Scheme (FRGS) by Malaysian Ministry of Higher Education, grant number FRGS/1/2022/STG01/UKM/01/2 awarded to Zamri Zainal by Universiti Kebangsaan Malaysia (UKM).

Declarations

Competing interests

The authors declare no competing interests.

Additional information

Supplementary Information The online version contains supplementary material available at <https://doi.org/10.1038/s41598-025-92942-5>.

Correspondence and requests for materials should be addressed to M.-R.A.-Z. or Z.Z.

Reprints and permissions information is available at www.nature.com/reprints.

Publisher's note Springer Nature remains neutral with regard to jurisdictional claims in published maps and institutional affiliations.

Open Access This article is licensed under a Creative Commons Attribution-NonCommercial-NoDerivatives 4.0 International License, which permits any non-commercial use, sharing, distribution and reproduction in any medium or format, as long as you give appropriate credit to the original author(s) and the source, provide a link to the Creative Commons licence, and indicate if you modified the licensed material. You do not have permission under this licence to share adapted material derived from this article or parts of it. The images or other third party material in this article are included in the article's Creative Commons licence, unless indicated otherwise in a credit line to the material. If material is not included in the article's Creative Commons licence and your intended use is not permitted by statutory regulation or exceeds the permitted use, you will need to obtain permission directly from the copyright holder. To view a copy of this licence, visit <http://creativecommons.org/licenses/by-nc-nd/4.0/>.

© The Author(s) 2025